

UC San Diego

UC San Diego Previously Published Works

Title

BMP receptor blockade overcomes extrinsic inhibition of remyelination and restores neurovascular homeostasis

Permalink

<https://escholarship.org/uc/item/80f2s36g>

Journal

Brain, 144(8)

ISSN

0006-8950

Authors

Petersen, Mark A
Tognatta, Reshmi
Meyer-Franke, Anke
et al.

Publication Date

2021-09-04



DOI

10.1093/brain/awab106

Peer reviewed



BMP receptor blockade overcomes extrinsic inhibition of remyelination and restores neurovascular homeostasis

Mark A. Petersen,^{1,2,3,†} Reshmi Tognatta,^{1,2,†} Anke Meyer-Franke,^{1,2} Eric A. Bushong,⁴  Andrew S. Mendiola,^{1,2} Zhaoqi Yan,^{1,2}  Abinaya Muthusamy,² Mario Merlini,² Rosa Meza-Acevedo,^{1,2} Belinda Cabriga,^{1,2} Yungui Zhou,^{1,2} Reuben Thomas,² Jae Kyu Ryu,^{1,2,5} Hans Lassmann,⁶ Mark H. Ellisman^{4,7} and Katerina Akassoglou^{1,2,5}

[†]These authors contributed equally to this work.

Extrinsic inhibitors at sites of blood–brain barrier disruption and neurovascular damage contribute to remyelination failure in neurological diseases. However, therapies to overcome the extrinsic inhibition of remyelination are not widely available and the dynamics of glial progenitor niche remodelling at sites of neurovascular dysfunction are largely unknown.

By integrating *in vivo* two-photon imaging co-registered with electron microscopy and transcriptomics in chronic neuroinflammatory lesions, we found that oligodendrocyte precursor cells clustered perivascularly at sites of limited remyelination with deposition of fibrinogen, a blood coagulation factor abundantly deposited in multiple sclerosis lesions. By developing a screen (OPC-X-screen) to identify compounds that promote remyelination in the presence of extrinsic inhibitors, we showed that known promyelinating drugs did not rescue the extrinsic inhibition of remyelination by fibrinogen. In contrast, bone morphogenetic protein type I receptor blockade rescued the inhibitory fibrinogen effects and restored a promyelinating progenitor niche by promoting myelinating oligodendrocytes, while suppressing astrocyte cell fate, with potent therapeutic effects in chronic models of multiple sclerosis.

Thus, abortive oligodendrocyte precursor cell differentiation by fibrinogen is refractory to known promyelinating compounds, suggesting that blockade of the bone morphogenetic protein signalling pathway may enhance remyelinating efficacy by overcoming extrinsic inhibition in neuroinflammatory lesions with vascular damage.

1 Gladstone UCSF Center for Neurovascular Brain Immunology, San Francisco, CA 94158, USA

2 Gladstone Institutes, University of California, San Francisco, CA 94158, USA

3 Department of Pediatrics, University of California, San Francisco, CA 94143, USA

4 National Center for Microscopy and Imaging Research, Center for Research on Biological Systems, University of California, San Diego, La Jolla, CA 92093, USA

5 Department of Neurology, Weill Institute for Neurosciences, University of California, San Francisco, CA 94158, USA

6 Center for Brain Research, Medical University of Vienna, A-1090 Vienna, Austria

7 Department of Neurosciences, University of California, San Diego, La Jolla, CA 92093, USA

Correspondence to: Katerina Akassoglou, PhD

Gladstone Institutes, 1650 Owens Street

San Francisco, CA 94158, USA

E-mail: kakassoglou@gladstone.ucsf.edu

Received December 07, 2020. Revised March 01, 2021. Accepted March 02, 2021

© The Author(s) (2021). Published by Oxford University Press on behalf of the Guarantors of Brain.

This is an Open Access article distributed under the terms of the Creative Commons Attribution Non-Commercial License (<http://creativecommons.org/licenses/by-nc/4.0/>), which permits non-commercial re-use, distribution, and reproduction in any medium, provided the original work is properly cited. For commercial re-use, please contact journals.permissions@oup.com

Keywords: multiple sclerosis; blood-brain barrier; promyelinating drugs; neuroinflammation; RNA sequencing

Abbreviations: BMP = bone morphogenetic protein; EAE = experimental autoimmune encephalomyelitis; OPC = oligodendrocyte precursor cell; SBEM = serial block face electron microscopy

Introduction

Regeneration of CNS myelin fails in several neurological diseases, including multiple sclerosis, neonatal brain injury and stroke.¹ In these conditions, cell-extrinsic cues in the microenvironment inhibit remyelination by blocking multipotent oligodendrocyte precursor cells (OPCs) from differentiating into mature, myelin-producing oligodendrocytes.² A critical barrier to therapeutic advances in chronic demyelinating diseases such as multiple sclerosis is the inability to overcome this inhibitory lesion environment and halt disease progression.^{3,4} Small molecules that enhance the intrinsic pathways of OPC differentiation and remyelination have been identified in drug screens.^{5–9} However, these drugs have failed to overcome disease-relevant extrinsic inhibitors of OPC differentiation such as chondroitin sulfate proteoglycans (CSPGs) and inflammatory cytokines and fail to promote oligodendrocyte differentiation in aged OPCs.^{10–12} Whether promyelinating compounds can overcome the inhibitory microenvironment at sites of increased vascular permeability remains unknown.

In multiple sclerosis, blood–brain barrier disruption allows the blood coagulation factor fibrinogen to enter the CNS.¹³ Fibrinogen deposition is one of the earliest events in multiple sclerosis pathogenesis and persists in chronically demyelinated lesions but is minimal in remyelinated lesions.^{14–16} In progressive multiple sclerosis, fibrinogen is detected in the cortex and CSF and correlates with neuronal and cortical loss.^{17,18} In demyelinating models, genetic or pharmacological depletion of fibrinogen promotes remyelination.^{14,19} Fibrinogen activates bone morphogenetic protein (BMP) receptor signalling in OPCs and neural precursor cells to inhibit remyelination and neurogenesis, respectively.^{14,20} Fibrinogen induces a cell fate switch of NG2⁺ (encoded by CSPG4) OPCs to astrocytes via BMP receptor activation,¹⁴ suggesting a role for fibrinogen in the extrinsic inhibition of remyelination by inducing OPC-derived astrogenesis in the neurovascular niche. Furthermore, when fibrinogen is converted to fibrin, it induces oxidative stress and pro-inflammatory polarization of microglia and macrophages,^{21,22} which is toxic to OPCs and contributes to remyelination failure.^{23,24} This suggests a critical role for increased vascular permeability and fibrinogen deposition in the maintenance of an inhibitory microenvironment in chronic neurological diseases. However, the remodelling of the neurovascular niche at sites of blood–brain barrier disruption and its relationship with remyelination failure remains poorly understood.

Here, we show that the extrinsic inhibition of remyelination by fibrinogen activates signalling pathways in OPCs that could not be overcome by known promyelinating compounds. In contrast, inhibition of the BMP type I receptor rescued the inhibitory effects of fibrinogen on remyelination by restoring the cell fate of OPCs to mature oligodendrocytes with therapeutic effects in chronic models of experimental autoimmune encephalomyelitis (EAE). By integrating transcriptomics with *in vivo* two-photon imaging co-registered with electron microscopy in chronic neuroinflammatory lesions, we show that OPCs accumulate at sites of fibrinogen deposition with active BMP signalling and limited remyelination. Thus, known promyelinating compounds do not overcome BMP

receptor activation and abortive OPC differentiation by fibrinogen, suggesting that BMP pathway inhibition may enhance the regenerative potential of the promyelinating progenitor niche at sites of cerebrovascular damage.

Materials and methods

Detailed methods are provided in the [Supplementary material](#).

Animals

All animal protocols were approved by the Committee of Animal Research at the University of California, San Francisco, and in accordance with the National Institutes of Health and ARRIVE guidelines.

Data availability

The raw data files from the bulk RNA-sequencing (RNA-seq) are deposited in the Gene Expression Omnibus under GEO: GSE166675. The raw data from serial block face electron microscopy (SBEM) are deposited in the Cell Image Library under <http://cellimagelibrary.org/groups/54355>. Other study data are available from the corresponding author, upon reasonable request.

Results

NG2 cells cluster perivascularly at sites of fibrinogen deposition with limited remyelination

NG2 cells, also referred to as OPCs, are progenitor cells in the adult CNS closely associated with the vasculature with unique potential to promote remyelination.²⁵ To study NG2 cells and neurovascular dysfunction in neuroinflammation, we generated NG2-CreERTM; Rosa^{tdTomato/+}; Cx3cr1^{GFP/+} mice. We performed *in vivo* two-photon imaging and transcriptomic profiling of NG2 cells and microglia during chronic EAE induced by the epitope of amino acids 35–55 of myelin oligodendrocyte glycoprotein (MOG_{35–55} EAE) ([Supplementary Fig. 1](#)). We used extravasation of 70 kDa Oregon GreenTM Dextran as a marker of acute blood–brain barrier leakage, and fibrinogen immunohistology as a marker of chronic blood–brain barrier leakage and local coagulation. At peak EAE, perivascular clusters consisted primarily of microglia, and NG2 cells were evenly distributed in the spinal cord parenchyma ([Fig. 1A](#) and [Supplementary Fig. 2A](#)). However, in chronic EAE, perivascular clusters also consisted of NG2 cells, with more than ~80% of NG2 cell clusters located at or within 30 μm of a blood vessel ([Fig. 1A](#), [Supplementary Fig. 2B](#) and [Supplementary Video 1](#)). NG2^{tdTomato+} cells in the clusters had glial-like morphology characterized by multiple branched processes in the spinal cord parenchyma, distinguishable from NG2^{tdTomato+} pericytes with elongated processes along the blood vessel wall ([Supplementary Fig. 2C](#)). Fibrinogen is deposited around leaky blood vessels and is necessary for EAE pathogenesis.^{26–28} Acute dextran leakage was highest at peak EAE, while fibrinogen deposition increased over time and was highest at chronic EAE ([Fig. 1B](#)). Sustained fibrinogen detection is consistent with impaired fibrinolysis and fibrin deposition in multiple sclerosis lesions.¹³ Endothelial

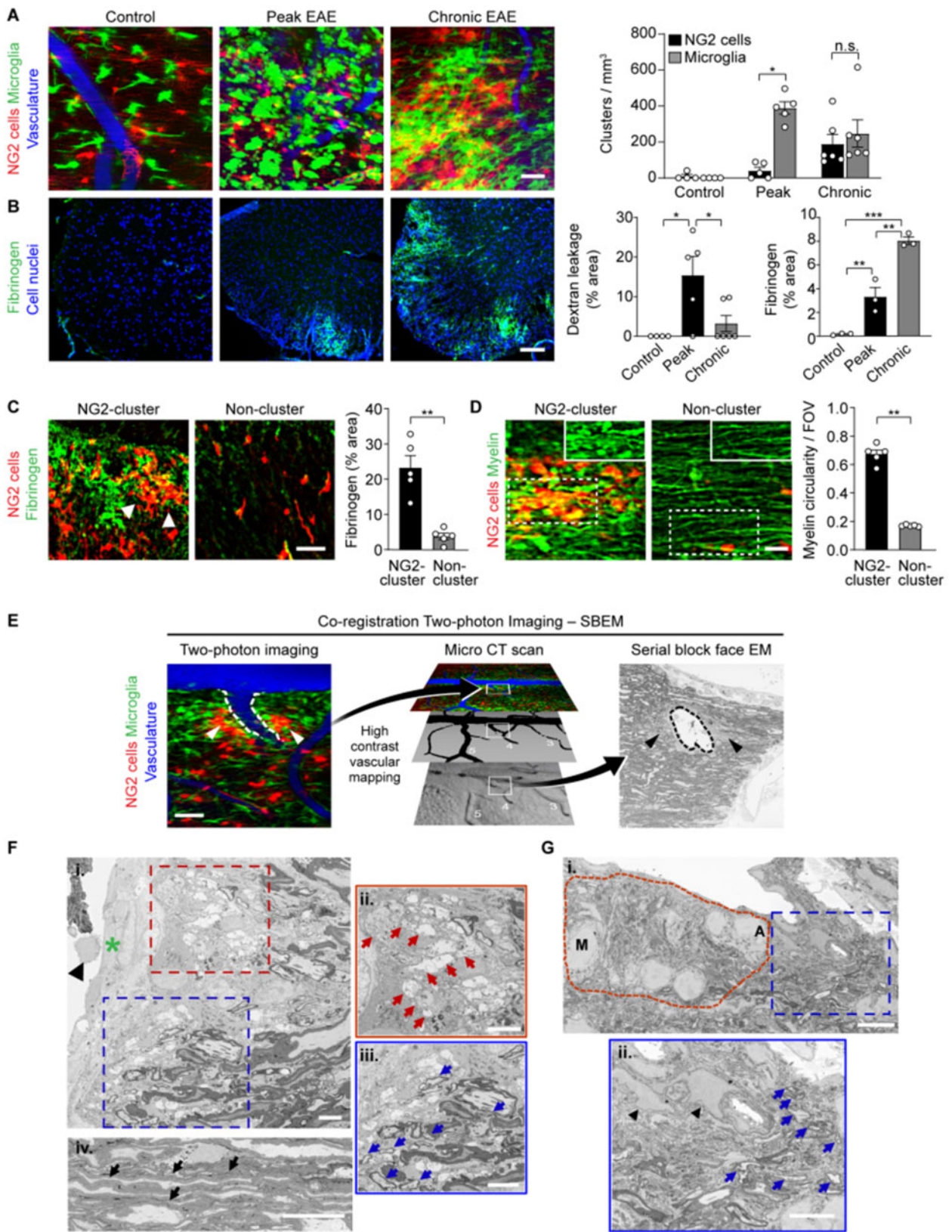


Figure 1 NG2 cells cluster perivascularly at sites of fibrinogen deposition and limited remyelination in chronic neuroinflammation. (A) *In vivo* two-photon maximum intensity projection images of microglia (green), NG2 cells (red) and the vasculature (blue, 70 kDa Oregon Green™ Dextran) in NG2-CreERTM; Rosa^{tdTomato/+}; Cx3cr1^{GFP/+} age-matched healthy control mice at the peak of clinical signs (peak EAE, mean score 3) and at chronic EAE (mean clinical score 2.1). Images shown are from mice on Days 17 (peak) and 35 (chronic) after the induction of EAE. Scale bar = 50 μm. Quantification of NG2 cells and microglial clusters in control (n = 4 mice), peak (n = 5 mice) and chronic (n = 6 mice) EAE. Values are mean ± SEM, *P < 0.05, n.s. = not significant (two-way ANOVA with Bonferroni's multiple comparisons test). (B) Microscopy of spinal cord sections from unimmunized healthy mice (control) and MOG₃₅₋₅₅-EAE mice at peak and chronic stages of disease immunostained for fibrinogen (green). Nuclei are stained with 4',6-diamidino-2-

(continued)

cell activation in peak and chronic EAE white matter lesions was shown with increased VCAM1 and PLVAP, a marker of endothelial fenestrae in leaky CNS vessels,²⁹ as well as ultrastructural analysis (Supplementary Fig. 3). In chronic EAE, NG2 clusters aggregated perivascularly only at sites of fibrinogen deposition (Fig. 1C and Supplementary Fig. 4A) and often co-localized with microglial clusters (Fig. 1A and Supplementary Fig. 2A). These results suggest dynamic glial remodelling of the neurovascular interface at sites of fibrinogen deposition during neuroinflammation.

To assess myelin within perivascular NG2 clusters using *in vivo* two-photon imaging, we applied MitoTracker[®] Deep Red, a lipophilic myelin label.³⁰ Significant myelin disruption, characterized by blebbing of myelin sheaths, was present near NG2 clusters, whereas normal-appearing myelin sheaths appeared at sites without clusters (Fig. 1D and Supplementary Fig. 4B). To study myelin ultrastructure at the perivascular NG2 clusters, we developed a method to co-register the two-photon-imaged volume in EAE mice with 3D SBEM using microcomputed tomography [Fig. 1E and Supplementary Video 2 (available from figshare, doi:10.6084/m9.figshare.14981190)]. We observed inflamed veins with endothelial activation, attachment of leucocytes at the endothelial surface, perivascular astrogliosis and inflammation, in part with debris-containing macrophages [Fig. 1F(i), G(i) and Supplementary Fig. 3C]. In the parenchymal lesions, we found two distinct patterns: the first was characterized by infiltration of elongated cells with low cell density, some of which contained osmiophilic degradation products. In these areas, axons were predominantly demyelinated, and remyelination was sparse [Fig. 1F(ii) and G(ii)]. In other areas, there were more dense clusters of small cells with small rims of perinuclear cytoplasm containing some mitochondria, but few other organelles, which were reminiscent of NG2 cells [Fig. 1G(ii)]. Remyelinated axons were closely adjacent to these cell clusters, while in areas distant from the clusters, axons were demyelinated [Fig. 1F(iii) and G(ii)]. Away from the perivascular NG2 cells, we observed normal-appearing perivascular CNS tissue, astrocytic glia limitans and axons with normal myelin thickness [Fig. 1F(iv)]. These results suggest that perivascular NG2 clusters are associated with inflammation, gliosis, frank demyelination and limited remyelination.

Transcriptomic profiling of NG2 cells reveals regulation of vascular, immune and coagulation pathways

To study the transcriptomic changes in NG2 cells in chronic EAE, we performed RNA-seq on NG2^{tdTomato+} cells collected from the spinal cords of MOG₃₅₋₅₅ EAE mice or healthy controls

(Supplementary Fig. 5A). We identified 1241 differentially expressed genes [false discovery rate (FDR) < 0.05; ± 1 log₂ fold change] in the setting of chronic EAE compared to the control, of which 738 were downregulated (60%) and 503 upregulated (40%) (Fig. 2A and Supplementary Table 1). Unsupervised gene clustering analysis identified nine distinct gene clusters (Fig. 2B and Supplementary Table 1). Gene ontology (GO) analysis revealed that chronic EAE activated inflammatory and antigen-presentation genes in clusters 1–4, including the GO pathway terms ‘Positive regulation of acute inflammatory response’, ‘Positive regulation of T cell mediated cytotoxicity’, ‘Antigen processing and presentation’ and ‘Cellular response to interferon-beta’ (Fig. 2B and Supplementary Table 1). Canonical antigen presentation genes such as *Cd74*, *H2-DMA* and *B2m* were significantly upregulated in EAE (Fig. 2B and Supplementary Table 1), which was consistent with reports suggesting immune-like functions of oligodendrocyte lineage cells in disease.^{31,32} Interestingly, GO analysis of downregulated gene clusters 5–9 revealed pathways related to vascular and blood–brain barrier homeostasis such as ‘Angiogenesis’, ‘Regulation of Wnt signaling pathway’, ‘Vasculogenesis’, ‘Blood vessel development’ and ‘Cell junction organization’ (Fig. 2B and Supplementary Table 1). In accordance, gene networks involved in ‘Blood vessel maintenance’, ‘Wound healing and blood coagulation’ and ‘Tight junctions’ were globally repressed in EAE (Fig. 2C and Supplementary Table 2). Gene set enrichment analysis of differentially expressed genes identified the top two downregulated gene sets as ‘Regulation of cell junction assembly’ (normalized enrichment score = 1.7, *P* < 0.01) and ‘Negative regulation of coagulation’ (normalized enrichment score = 1.7, *P* < 0.01) (Fig. 2D and Supplementary Table 2). Expression of tissue factor pathway inhibitor (*Tfpi*), an inhibitor of blood coagulation and fibrin formation,³³ was significantly reduced in NG2 cells in EAE (Supplementary Table 1). As expected, the NG2^{tdTomato+} population included OLIG2⁺ oligodendrocyte lineage cells and PDGFRβ⁺ pericytes (Supplementary Fig. 6). We isolated PDGFRα⁺ and PDGFRβ⁺ cells from the spinal cords of MOG₃₅₋₅₅-EAE mice or healthy controls (Supplementary Fig. 5B) and labelled cell surface major histocompatibility complex (MHC) class II and TFPI to assess the antigen presentation and anticoagulation pathways, respectively. Consistent with our bulk-RNAseq and prior studies,³² MHC class II was increased in PDGFRα⁺ cells in EAE (Supplementary Fig. 5C). TFPI was expressed in PDGFRα⁺ cells in healthy controls and was repressed in EAE (Supplementary Fig. 5D). Overall, these results identify dysregulation of antigen presentation, coagulation and vascular homeostasis pathways in NG2 cells in chronic neuroinflammation.

Figure 1 Continued

phenylindole (DAPI, blue). Scale bar = 100 μm. Quantification of dextran leakage in spinal cord of unimmunized, healthy mice (control) (*n* = 4 mice) and MOG₃₅₋₅₅-EAE mice at peak (*n* = 5 mice) and chronic (*n* = 6 mice) stages of disease. Values are mean ± SEM, **P* < 0.05 (one-way ANOVA with Tukey’s multiple comparisons test). Quantification of fibrinogen immunoreactivity in spinal cord of unimmunized healthy mice (control) and MOG₃₅₋₅₅-EAE mice at peak and chronic stages of disease (*n* = 3 mice per group). Values are mean ± SEM, ***P* < 0.01, ****P* < 0.001 (one-way ANOVA with Tukey’s multiple comparisons test). (C) Microscopy of ventral spinal cord sections of NG2-CreERTM;Rosa^{tdTomato/+};Cx3cr1^{GFP/+} mice at chronic EAE immunostained for fibrinogen (green). Scale bar = 50 μm. Quantification of fibrinogen immunopositivity in areas of NG2 clusters and areas without clusters (*n* = 5 mice). Values are mean ± SEM, ***P* < 0.01 (two-tailed Mann-Whitney test). (D) *In vivo* two-photon maximum intensity projection images of myelin (green) in NG2-CreERTM;Rosa^{tdTomato/+};Cx3cr1^{GFP/+} mice at chronic EAE in areas of NG2 clusters and areas without clusters. Myelin (green channel) of dotted line box is shown in the inset. Scale bar = 20 μm. Quantification of myelin damage at chronic EAE in areas with and without NG2 clusters (*n* = 5 mice). Values are mean ± SEM, ***P* < 0.01 (two-tailed Mann-Whitney test). FOV = field of view. (E) Region of interest tracking workflow for the co-registration of two-photon and SBEM volumes. Dotted lines indicate co-registered blood vessels. Arrowheads indicate co-registered NG2 clusters. (F and G) Representative co-registered SBEM images from *n* = 3 regions of interest from two different mice. [F(i–iii)] CNS parenchyma in areas of NG2 clusters shows an inflamed spinal cord vessel with activated endothelial cells (green asterisk), attachment of a leucocyte to the endothelium (black arrowhead) and perivascular lesions with dominant demyelination (red boxed area) and sparse remyelination (blue boxed area). Red arrows depict demyelinated axons. Blue arrows depict remyelinated axons. Scale bars = 20 μm in F(i); 10 μm in F(ii and iii). [F(iv)] Correlated SBEM within the CNS parenchyma in an area without NG2 clusters. Black arrows depict normal myelinated axons. Scale bar = 10 μm. [G(i and ii)] Representative SBEM from a region of interest in an area of NG2 clusters with perivascular demyelination. Infiltrating macrophage (M) and astrocyte (A) in an area of gliosis (red dotted area) and limited remyelination (blue boxed area). Blue arrows indicate remyelinated axons. Black arrowheads indicate NG2 cells. Scale bars = 10 μm in G(i); 5 μm G(ii).

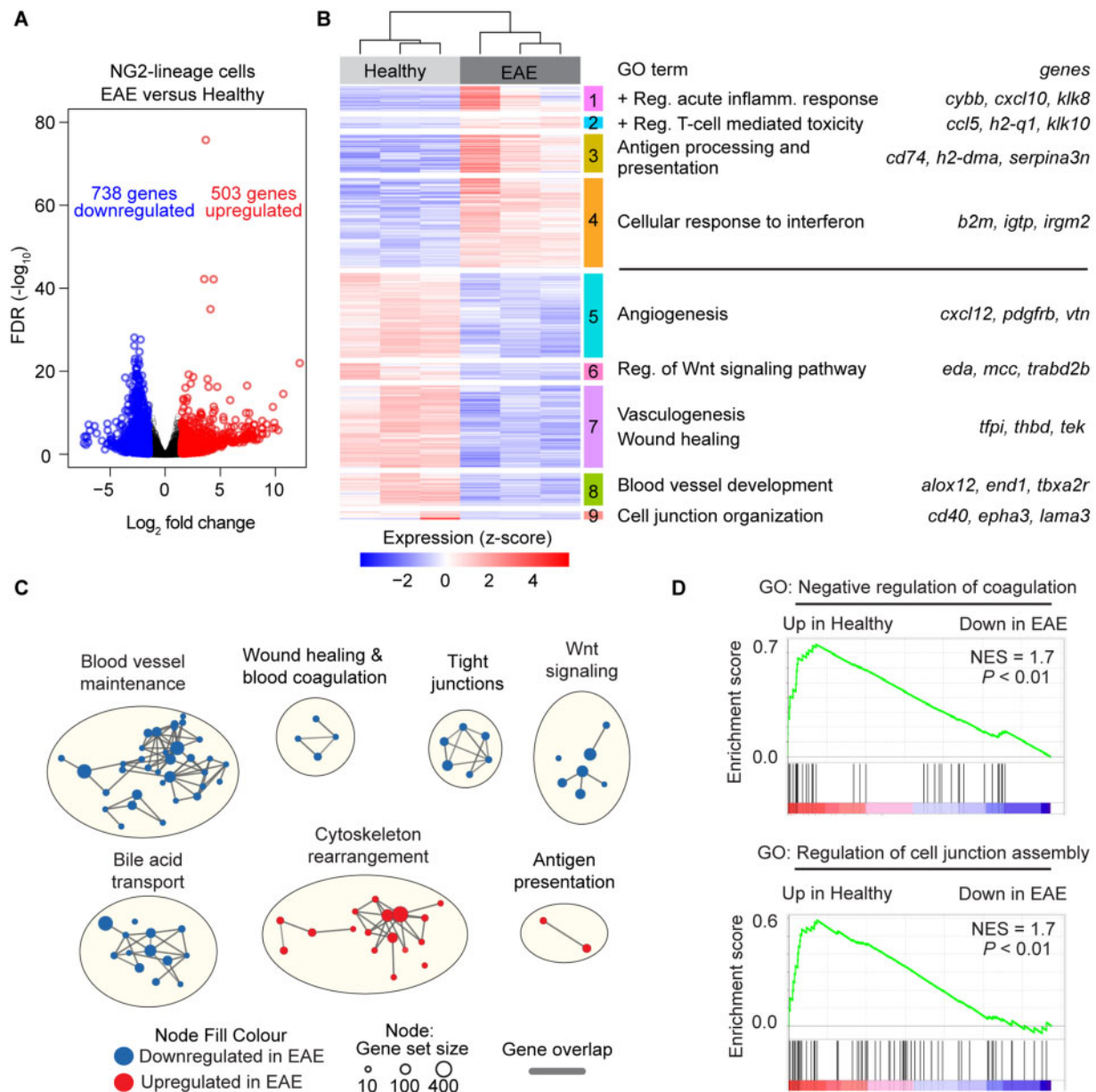


Figure 2 RNA-seq analysis of NG2 cells in EAE. (A–D) Data are from $n = 3$ mice per group. (A) Volcano plot of differentially expressed genes from RNA-seq analysis of NG2 lineage cells from MOG_{35–55}-EAE or healthy mice. Circles depict genes significantly downregulated (blue; log₂ fold change < -1; FDR < 0.05) or upregulated (red; log₂ fold change > 1; FDR < 0.05) in EAE compared to healthy mice. (B) Heat map of data from A. Genes were clustered by HOPACH unsupervised clustering analysis (clusters 1–9). Expression values were log normalized, row centred and depicted as a z-score. Significant GO terms and example genes are shown for each cluster. FDR < 0.05; Benjamini-Hochberg correction. (C) Visualization of co-expression GO term networks downregulated (blue nodes) or upregulated (red nodes) in NG2 cells from EAE compared to healthy mice. Gene set size and co-expression overlap (key) was determined by gene set enrichment analysis, $P < 0.05$. (D) Enrichment plot for the gene sets ‘Negative regulation of coagulation’ and ‘Regulation of cell junction assembly’ determined by gene set enrichment analysis of RNA-seq data of NG2 cells from EAE or healthy mice. The x-axis shows the gene rank in the dataset. NES = normalized enrichment score.

Promyelinating compounds do not overcome fibrinogen extrinsic inhibition of OPC differentiation

OPCs can differentiate to myelinating oligodendrocytes or astrocyte-like cells in response to extrinsic signals found in multiple sclerosis lesions like fibrinogen or BMPs.^{14,34,35} We developed the OPC-X-screen, a medium-throughput, high-content imaging assay to identify compounds that in the presence of extrinsic inhibitors promote OPC differentiation to mature MBP⁺ oligodendrocytes and decrease the OPC fate-switch to GFAP⁺ astrocytes (Fig. 3A). In the OPC-X assay, fibrinogen decreased MBP⁺ mature oligodendrocytes and increased GFAP⁺ astrocyte-like cells by ~60% compared

with the controls (Fig. 3B). Seven compounds—benztropine, clemastine, quetiapine, miconazole, clobetasol, (±)U-50488 and XAV-939—have previously been identified to promote intrinsic pathways of OPC differentiation.^{5–8} However, these promyelinating compounds did not overcome the extrinsic inhibition of OPC differentiation by fibrinogen (Fig. 3B). In contrast, the BMP type I receptor inhibitor DMH1³⁶ rescued the inhibitory effects of fibrinogen and restored OPC differentiation to mature oligodendrocytes to control levels (Fig. 3B). The cell-fate switch of OPCs to GFAP⁺ cells by fibrinogen was also abolished by DMH1 (Fig. 3B). Clemastine, a muscarinic receptor antagonist, promotes the

remyelinating potential of OPCs and is currently in clinical trials for multiple sclerosis.^{6,37} While clemastine increased the number of MBP⁺ cells in control conditions as expected, it did not enhance OPC differentiation to mature oligodendrocytes in the presence of fibrinogen (Supplementary Fig. 7A). Clemastine did not block fibrinogen-induced phosphorylation of the BMP signal transducers SMAD1/5 or expression of the BMP target protein ID2 (Fig. 3C). In contrast, DMH1 blocked fibrinogen-induced SMAD1/5 phosphorylation and ID2 expression (Fig. 3C). Thus, previously-identified compounds promoting OPC differentiation may not overcome extrinsic inhibition signalling pathways at sites of vascular damage.

Therapeutic effects of type I BMP receptor inhibition in neuroinflammation

BMP expression and downstream receptor signalling is increased in human multiple sclerosis lesions.³⁸ The BMP target protein ID2 is also increased in lesions with extensive fibrinogen deposition.¹⁴ The finding that DMH1 effectively blocked fibrinogen-induced BMP receptor activation and restored OPC differentiation *in vitro* (Fig. 3) suggested that targeting BMP signalling may promote repair in neuroinflammation. However, DMH1 is not water-soluble, which limits its use *in vivo*. Therefore, we tested LDN-212854, a water-soluble activin A receptor type I (ACVR1)-biased type I BMP receptor inhibitor with a molecular structure similar to DMH1,³⁹ in the OPC-X-Screen. LDN-212854 restored mature oligodendrocyte differentiation and blocked the formation of GFAP⁺ astrocytes from fibrinogen-treated OPCs in a dose-dependent manner (Fig. 3D). While in the presence of fibrinogen, clemastine alone had no effect on OPC differentiation. Clemastine increased MBP⁺ cells by 4.8-fold in combination with LDN-212854 compared to a 3.7-fold increase with LDN-212854 alone (Supplementary Fig. 7B), suggesting that the effects of LDN-212854 on OPC differentiation to MBP⁺ cells may be increased with promyelinating drugs. Clemastine had no effect on OPC differentiation to astrocytes either alone or in combination with LDN-212854 (Supplementary Fig. 7B). Thus, BMP receptor inhibition may restore the cell fate of OPCs to mature oligodendrocytes in the presence of extrinsic inhibition, while limiting the generation of GFAP⁺ cells in neuroinflammatory lesions with fibrinogen deposition and active BMP signalling.

To determine the therapeutic potential of LDN-212854 and its effects on the OPC niche and BMP pathway activation *in vivo*, we selected two models of EAE: chronic MOG_{35–55} EAE induced in NG2-CreERTM:Rosa^{tdTomato/+} mice and progressive EAE induced in non-obese diabetic mice by the epitope of amino acids 35–55 of MOG. Therapeutic administration of LDN-212854 significantly improved clinical scores and reduced fibrinogen deposition and demyelination in both models (Fig. 4A–D). LDN-212854 also markedly reduced perivascular NG2 clusters and myelin damage in MOG_{35–55} EAE mice, as revealed by *in vivo* two-photon imaging (Fig. 4E and F). Moreover, LDN-212854 decreased ID2 expression in NG2 cells in the EAE white matter lesions (Fig. 4G), consistent with the inhibition of BMP signalling in the NG2 cell lineage. Since a key mechanism of fibrinogen and BMP receptor signalling is the cell fate switch of OPCs to astrocytes,^{14,35} we tested whether LDN-212854 promoted OPC differentiation to myelinating cells in MOG_{35–55} EAE mice. To trace the cell fate of OPCs *in vivo*, we induced EAE in the NG2-CreERTM:Rosa^{tdTomato/+} mice, allowing tamoxifen-induced expression of tdTomato in NG2⁺ OPCs and their progeny.^{14,34} Glutathione S-transferase-pi (GST-pi)-labelled mature oligodendrocytes and GFAP-labelled astrocytes derived from genetically-labelled tdTomato⁺ NG2⁺ OPCs. Therapeutic administration of LDN-212854 increased the proportion NG2^{tdTomato+} OPCs that differentiated into GST-pi⁺ mature oligodendrocytes compared with the controls and abolished the formation of OPC-derived GFAP⁺

astrocytes in NG2-CreERTM:Rosa^{tdTomato/+} MOG_{35–55} EAE mice (Fig. 4H). Collectively, these results suggest that BMP receptor inhibition may be utilized to direct the OPC niche towards myelinating oligodendrocytes, while limiting gliosis at sites of cerebrovascular damage in neuroinflammatory diseases.

Discussion

Our study reveals the dynamic cellular remodelling of the neurovascular niche at sites of blood–brain barrier dysfunction in neuroinflammation and identifies a druggable pathway to promote myelin repair. Our working model is that in neuroinflammation, perivascular NG2⁺ cell clusters regulate immune and blood coagulation pathways leading to excessive fibrin deposition, activation of BMP receptor signalling in OPCs and extrinsic inhibition of remyelination at sites of vascular damage. This model is consistent with chronically demyelinated multiple sclerosis lesions, in which perivascular OPC clusters are localized in the active lesion borders with fibrinogen deposition, impaired fibrinolysis, BMP pathway activation and gliosis.^{14,15,17,29} Through the OPC-X-screen, we discovered that the therapeutic potential of many promyelinating drugs may be limited at sites of vascular damage and fibrinogen deposition, highlighting the unmet clinical need for therapeutic strategies to overcome extrinsic inhibition in diseases with chronic demyelination. Importantly, we introduce the concept that inhibiting BMP pathway activation may promote myelin repair by overcoming abortive OPC differentiation at sites of neurovascular dysfunction. Thus, BMP inhibitors could expand the toolbox of promyelinating drugs and provide additional therapeutic options for patients with blood–brain barrier disruption and white matter pathology.

Using *in vivo* two-photon imaging, we found a striking transition of the perivascular glial cell composition associated with microglia and demyelination at the peak of disease, followed by the formation of perivascular NG2 clusters with limited remyelination in chronic neuroinflammation. Oligodendroglia closely interact with the developing vasculature⁴⁰ and bi-directional OPC–endothelial cell interactions may regulate myelination and white matter vascularization.^{29,41} It is possible that fibrinogen deposition at sites of perivascular OPC clusters may perturb OPC–endothelial cell crosstalk and alter cellular functions including OPC migration and maturation as well as endothelial cell proliferation and local coagulation. Our study suggests previously unknown functions of NG2 cells in the expression of genes regulating coagulation. TFPI, a potent inhibitor of coagulation factor X and tissue factor-mediated coagulation,³³ was repressed in chronic neuroinflammation. Interestingly, multiple sclerosis patients have alterations in haemostasis biomarkers including TFPI,⁴² suggesting an imbalance in anti- and procoagulant pathways in neuroinflammatory disease. Pro-oxidant microglia may also contribute to the procoagulant milieu in the lesion microenvironment through expression of coagulation proteins such as coagulation factor X.²² Thus, transcriptional changes at the neurovascular interface may establish a local procoagulant environment that contributes to the excessive or persistent deposition of fibrin observed in many neurological diseases.¹³ Therapeutic strategies to target the NG2 cell-vascular-fibrinogen axis or downstream fibrinogen signalling may provide a therapeutic avenue to overcome extrinsic inhibition in the neuroinflammatory lesion environment.

Our study suggests that promyelinating drugs differentially suppress signalling pathways activated by extrinsic inhibitors in the lesion environment. Activation of BMP signalling in the injured perivascular niche by fibrinogen directs OPC cell fate towards astrocytes rather than remyelinating oligodendrocytes,¹⁴ which may contribute to the inhibition of remyelination and pathologic

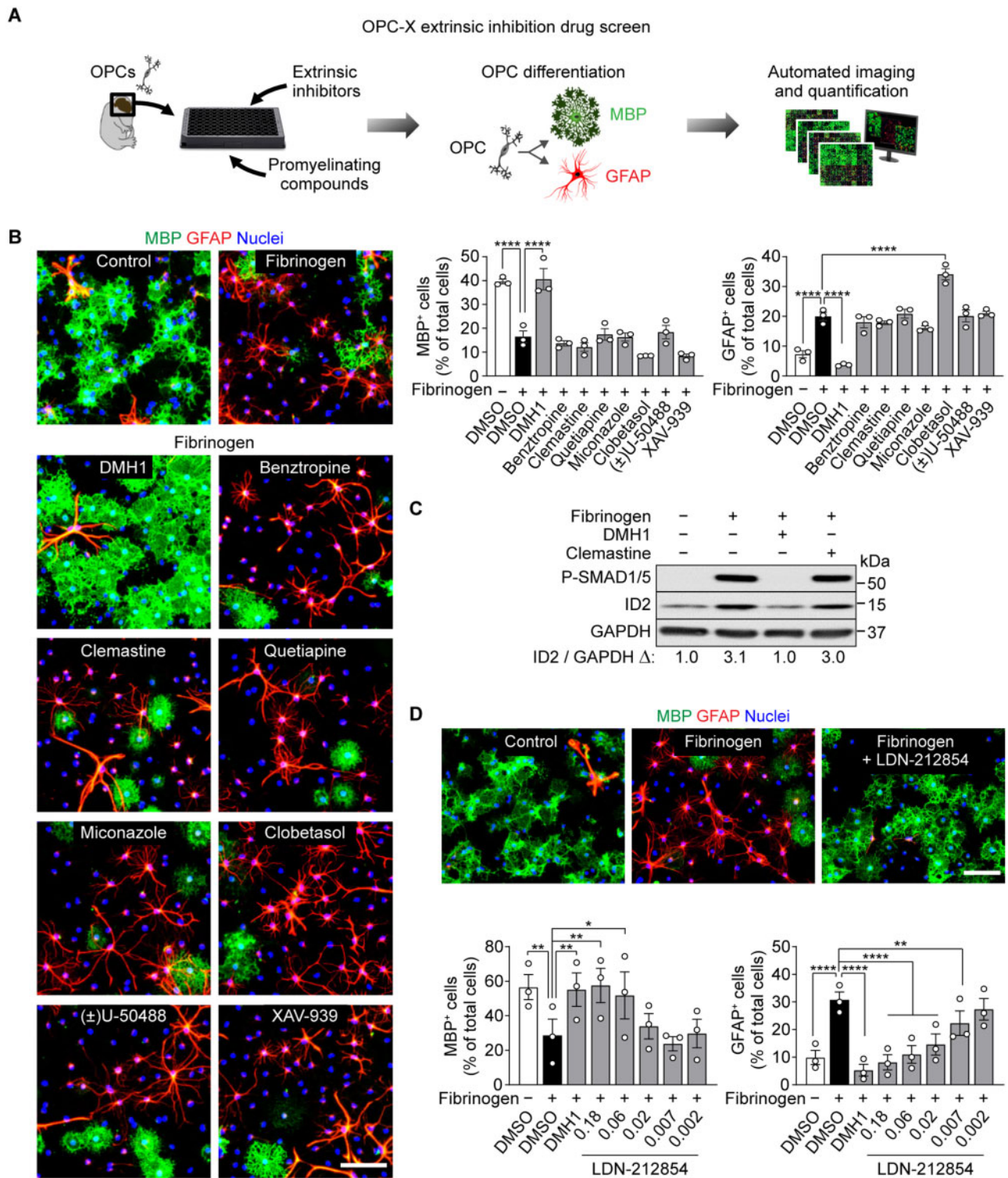


Figure 3 Promyelinating compounds do not overcome fibrinogen extrinsic inhibition of OPC differentiation. (A) Workflow for medium throughput, OPC-X screen of promyelinating drugs in the presence of fibrinogen. (B) Immunofluorescence for MBP (green) and GFAP (red) in primary rat OPCs treated with fibrinogen and myelin-promoting drugs or vehicle control (dimethylsulfoxide, DMSO) as indicated. Nuclei are stained with Hoechst dye (blue). Scale bar = 100 μm. Automated image acquisition and quantification of MBP⁺ and GFAP⁺ cells. Data are mean ± SEM from n = 3 independent experiments. ****P < 0.0001 (one-way ANOVA with Dunnett’s multiple comparisons test). (C) Phospho-SMAD1/5 (P-SMAD1/5) and ID2 protein levels in control or fibrinogen-treated primary rat OPCs in the presence of DMH1 or clemastine. Values are the mean of n = 3 independent experiments. (D) Immunofluorescence for MBP (green) and GFAP (red) in primary rat OPCs treated with fibrinogen and LDN-212854 (0.18 μM) or vehicle control (DMSO) for 3 days. Nuclei are stained with Hoechst dye (blue). Scale bar = 100 μm. Automated image acquisition and quantification of MBP⁺ and GFAP⁺ cells. Data are mean ± SEM from n = 3 independent experiments. *P < 0.05, **P < 0.01, ***P < 0.001, ****P < 0.0001 (matched one-way ANOVA with Dunnett’s multiple comparisons test).

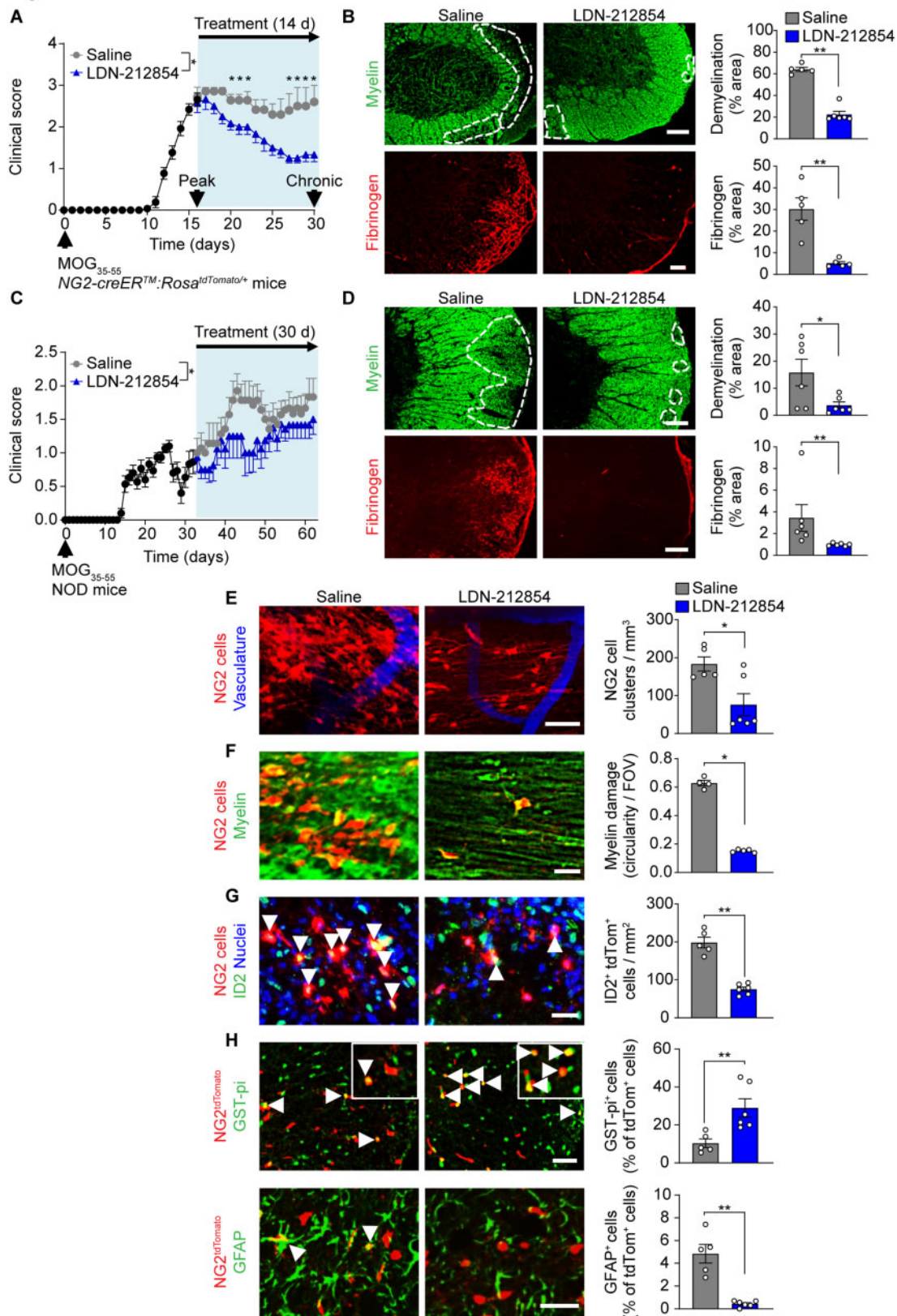


Figure 4 Therapeutic effects of type I BMP receptor inhibition in chronic neuroinflammation. (A) Clinical scores for MOG₃₅₋₅₅-EAE mice treated with LDN-212854 or saline (key) for 14 days starting at peak disease. Data are from $n = 6$ mice (EAE + LDN-212854) and $n = 5$ mice (EAE + saline), mean \pm SEM, $*P < 0.05$, (two-tailed permutation test). (B) Microscopy of spinal cord sections from MOG₃₅₋₅₅-EAE mice treated with saline (left) or LDN-212854 (right) immunostained for MBP to visualize myelin (green) and fibrinogen (red). Dashed line demarcates demyelinated white matter. Scale bar = 50 μ m. Quantification of demyelination and fibrinogen are shown. Data are from $n = 5-6$ mice per group, mean \pm SEM, $**P < 0.01$ (two-tailed Mann-Whitney test). (C) Clinical scores for non-obese diabetic-MOG₃₅₋₅₅ EAE mice treated with LDN-212854 or saline (key) for 30 days. Data are from $n = 8$

(continued)

gliosis at sites of vascular damage. Fibrinogen, in addition to activating BMP receptor signalling in OPCs, stimulates CSPG production from astrocytes and is a carrier for transforming growth factor- β .⁴³ CSPGs inhibit remyelination in part through the activation of the protein tyrosine phosphatase sigma receptor in OPCs.⁴⁴ Age-related loss of OPC function may occur in response to TGF- β signalling or increased stiffness in the OPC niche, with subsequent signalling through the mechanoresponsive ion channel PIEZO1.^{45,46} Therefore, assays that better recapitulate the inhibitory lesion environment and downstream signalling are needed to improve the selection of drugs that can increase remyelination in inflammatory lesions with gliosis, vascular damage and blood-brain barrier disruption. While other assays screen only for compounds promoting OPC differentiation to myelinating cells, the OPC-X-screen was developed with a dual readout of GFAP⁺ and MBP⁺ cells to identify compounds that suppress OPC cell fate switch to astrocytes and enhance myelination in the presence of extrinsic inhibitors. In the presence of fibrinogen, promyelinating drugs did not inhibit BMP receptor activation, or rescue OPC cell fate switch to astrocytes, or increase OPC differentiation to mature oligodendrocytes. These results suggest that BMP receptor inhibition may be needed *in vivo*, given that remyelination failure often occurs in areas of blood-brain barrier disruption and fibrinogen deposition.^{14–16} Thus, the choice of promyelinating drugs in the clinic may need to consider its efficacy within the extrinsic inhibitory milieu in patients with demyelinating neurological diseases. Drug combinations acting on distinct signalling pathways in OPCs may be required to promote remyelination in a broad range of patient populations.⁴⁷ The CCMR-Two clinical trial for multiple sclerosis plans to test clemastine combined with the diabetes drug metformin, which enhances the remyelinating potential of aged OPCs.¹¹ Future studies will determine the efficacy of BMP receptor inhibitors alone or in combination with promyelinating drugs to promote remyelination in multiple sclerosis and other neurological diseases with blood-brain barrier disruption and cerebrovascular damage.

Therapeutic fibrinogen depletion by anticoagulants can suppress neuroinflammation and promote myelin regeneration,¹³ but haemorrhagic complications may limit clinical use. Selective inhibition of fibrin's inflammatory functions by blocking fibrin interactions with its cell receptors or its intracellular pathways in immune cells has shown therapeutic benefits without anticoagulant effects.^{28,22,48} Our study identifies LDN-212854 as a selective ACVR1 inhibitor to overcome fibrinogen-induced BMP signalling in OPCs to promote remyelination. LDN-212854 increased myelinating oligodendrocytes and eliminated OPC differentiation to astrocytes in the presence of fibrinogen. Although BMP inhibition had a prominent effect on OPCs, we cannot rule out effects on other cell types such as endothelial cells, pericytes or inflammatory cells in

the CNS or periphery. Therapeutic administration of LDN-212854 at peak disease reduced demyelinated lesion size when compared to saline-treated animals, suggesting an anti-inflammatory effect of ACVR1 inhibition. The BMP family of proteins has immunomodulatory effects ranging from promoting T cell proliferation to maintaining regulatory T cells and suppressing antigen presenting capacity.^{49–51} Given that the BMP family regulates immune cell functions,⁵² we cannot exclude the anti-inflammatory effects of ACVR1 inhibition by LDN-212854 in addition to its promyelinating effect on OPCs. Future studies will determine the relative contributions of ACVR1 signalling in OPCs and inflammatory cells to myelin pathology in neurological diseases. Clinical use of ACVR1-selective BMP inhibitors has gained recent attention for the treatment of fibrodysplasia ossificans progressive, a rare disorder with overactive BMP signalling, resulting in heterotopic ossification and myelin abnormalities.⁵³ ACVR1 inhibitors have been safe and well-tolerated in phase I trials (Clinical Trial ID: NCT03429218; NCT03858075; ACTRN12619000319178) and are now moving into phase II trials for fibrodysplasia ossificans progressive and anaemia (Clinical Trial ID: NCT04307953; NCT04623996). LDN-212854, other safe ACVR1-selective inhibitors or modulators of the BMP receptor pathway may be added to the toolbox of promyelinating drugs as therapeutic options to overcome extrinsic inhibition of remyelination in neurological diseases with blood-brain barrier disruption and myelin abnormalities including multiple sclerosis, Alzheimer's disease, neonatal brain injury and traumatic brain injury.

Acknowledgements

We thank the Gladstone Flow Cytometry (N. Raman) and Genomics (M. Bernardi) Cores for expert technical assistance with flow cytometry, library preparations and sequencing. We thank A. Petraki for technical assistance, G. Maki for graphics and K. Claiborn for editorial assistance.

Funding

Gladstone Institutes was supported by the National Institutes of Health/National Center for Research Resources grant RR18928. The electron microscopy studies were carried out in the National Center for Microscopy and Imaging Research, which is supported by the National Institutes of Health grant P41 GM10341 (awarded to M.H.E.). M.A.P. was supported by research grants from the National Institutes of Health/National Institute of Neurological Disorders and Stroke K02 NS110973, National Multiple Sclerosis Society PP-1805-30887 and Race to Erase MS Foundation P0535497; A.S.M. by National Multiple Sclerosis Society Postdoctoral

Figure 4 Continued

mice (EAE + LDN-212854) and $n = 7$ mice (EAE + saline), mean \pm SEM, * $P < 0.05$, (Welch two-sample t-test comparing the group means of maximum scores, saline = 2.36, LDN-212854 = 1.75). NOD = non-obese diabetic. (D) Microscopy of spinal cord sections from non-obese diabetic-MOG_{35–55} EAE mice treated with saline (left) or LDN-212854 (right) with darkfield microscopy used to visualize myelin (green) and immunostained for fibrinogen (red). Dashed line demarcates demyelinated white matter. Scale bar = 100 μ m. Quantification of demyelination and fibrinogen are shown. Data are from $n = 6$ mice per group, mean \pm SEM, * $P < 0.05$ ** $P < 0.01$ (two-tailed Mann-Whitney test). (E) *In vivo* two-photon maximum intensity projection images of NG2 cells (red) and the vasculature (blue, 70 kDa Oregon GreenTM Dextran) in NG2-CreERTM:Rosa^{tdTomato/+} mice at chronic EAE treated with saline (left) and LDN-212854 (right). Scale bar = 50 μ m. Quantification of NG2 cell clusters is shown. Data are from $n = 6$ (EAE + LDN-212854) and $n = 5$ (EAE + saline), mean \pm SEM, * $P < 0.05$ (two-tailed unpaired t-test). (F) *In vivo* two-photon maximum intensity projection images of NG2 cells (red) and myelin (green, MitoTracker[®]) in NG2-CreERTM:Rosa^{tdTomato/+} mice at chronic EAE treated with saline (left) and LDN-212854 (right). Scale bar = 20 μ m. Image quantification of myelin damage is shown (right). Data are from $n = 5$ (EAE + LDN-212854) and $n = 4$ (EAE + saline), mean \pm SEM, * $P < 0.05$ (two-tailed Mann-Whitney test). (G) Microscopy of spinal cord sections from NG2-CreERTM:Rosa^{tdTomato/+} MOG_{35–55}-EAE mice after 14-day treatment of saline (left) or LDN-212854 (right). NG2 cells (red) and immunostaining for ID2 (green). Nuclei are stained with DAPI (blue). Scale bar = 25 μ m. Quantification of ID2⁺tdTom⁺ cells is shown. Data are from $n = 6$ (EAE + LDN-212854) and $n = 5$ (EAE + saline), mean \pm SEM, ** $P < 0.01$ (two-tailed Mann-Whitney test). (H) Fate mapping of tdTomato⁺ OPC-derived cells using microscopy of spinal cord sections from NG2-CreERTM:Rosa^{tdTomato/+} MOG_{35–55}-EAE mice after 14-day treatment of LDN-212854 or saline. NG2^{tdTomato+} cells (red) and immunostaining for the mature oligodendrocyte marker GST-pi (green, top) or the astrocyte marker GFAP (green, bottom). Scale bar = 50 μ m (top) and 20 μ m (bottom). Quantification of GST-pi and GFAP are shown. Data are from $n = 6$ (EAE + LDN-212854) and $n = 5$ (EAE + saline), mean \pm SEM, ** $P < 0.01$ (two-tailed Mann-Whitney test).

Fellowship FG-1708–28925, UCSF Immunology National Institutes of Health/National Institute of Allergy and Infectious Diseases T32AI007334 and the Berkelhammer Award for Excellence in Neuroscience; J.K.R. by National Multiple Sclerosis Society Postdoctoral Fellowship FG-1507–05496, Race to Erase MS Young Investigator Award and American Heart Association Scientist Development Grant 16SDG30170014. This work was supported by the Simon Family Trust, Edward and Pearl Fein, the Dagmar Dolby Family Fund, Conrad N. Hilton Foundation (17348), Department of Defense MS160082 and National Institutes of Health/National Institute of Neurological Disorders and Stroke R35 NS097976 to K.A.

Competing interests

K.A. is the scientific founder and advisor of Therini Bio, Inc. Her interests are managed by the Gladstone Institutes according to its conflict of interest policy.

Supplementary material

Supplementary material is available at *Brain* online.

References

- Franklin RJM, Ffrench-Constant C. Regenerating CNS myelin - from mechanisms to experimental medicines. *Nat Rev Neurosci*. 2017;18(12):753–769.
- Forbes TA, Gallo V. All wrapped up: Environmental effects on myelination. *Trends Neurosci*. 2017;40(9):572–587.
- Reich DS, Lucchinetti CF, Calabresi PA. Multiple sclerosis. *N Engl J Med*. 2018;378(2):169–180.
- Lubetzki C, Zalc B, Williams A, Stadelmann C, Stankoff B. Remyelination in multiple sclerosis: From basic science to clinical translation. *Lancet Neurol*. 2020;19(8):678–688.
- Mei F, Mayoral SR, Nobuta H, et al. Identification of the kappa-opioid receptor as a therapeutic target for oligodendrocyte remyelination. *J Neurosci*. 2016;36(30):7925–7935.
- Mei F, Fancy SPJ, Shen YA, et al. Micropillar arrays as a high-throughput screening platform for therapeutics in multiple sclerosis. *Nat Med*. 2014;20(8):954–960.
- Najm FJ, Madhavan M, Zaremba A, et al. Drug-based modulation of endogenous stem cells promotes functional remyelination in vivo. *Nature*. 2015;522(7555):216–220.
- Fancy SP, Harrington EP, Yuen TJ, et al. Axin2 as regulatory and therapeutic target in newborn brain injury and remyelination. *Nat Neurosci*. 2011;14(8):1009–1016.
- Deshmukh VA, Tardif V, Lyssiotis CA, et al. A regenerative approach to the treatment of multiple sclerosis. *Nature*. 2013;502(7471):327–332.
- Keough MB, Rogers JA, Zhang P, et al. An inhibitor of chondroitin sulfate proteoglycan synthesis promotes central nervous system remyelination. *Nat Commun*. 2016;7:11312.
- Neumann B, Baror R, Zhao C, et al. Metformin restores CNS remyelination capacity by rejuvenating aged stem cells. *Cell Stem Cell*. 2019;25(4):473–485.e8.
- Starost L, Lindner M, Herold M, et al. Extrinsic immune cell-derived, but not intrinsic oligodendroglial factors contribute to oligodendroglial differentiation block in multiple sclerosis. *Acta Neuropathol*. 2020;140(5):715–736.
- Petersen MA, Ryu JK, Akassoglou K. Fibrinogen in neurological diseases: Mechanisms, imaging and therapeutics. *Nat Rev Neurosci*. 2018;19(5):283–301.
- Petersen MA, Ryu JK, Chang KJ, et al. Fibrinogen activates BMP signaling in oligodendrocyte progenitor cells and inhibits remyelination after vascular damage. *Neuron*. 2017;96(5):1003–1012.e7.
- Lee NJ, Ha SK, Sati P, et al. Spatiotemporal distribution of fibrinogen in marmoset and human inflammatory demyelination. *Brain*. 2018;141(6):1637–1649.
- Vos CM, Geurts JJ, Montagne L, et al. Blood-brain barrier alterations in both focal and diffuse abnormalities on postmortem MRI in multiple sclerosis. *Neurobiol Dis*. 2005;20(3):953–960.
- Yates RL, Esiri MM, Palace J, Jacobs B, Perera R, DeLuca GC. Fibrin(ogen) and neurodegeneration in the progressive multiple sclerosis cortex. *Ann Neurol*. 2017;82(2):259–270.
- Magliozzi R, Hametner S, Facchiano F, et al. Iron homeostasis, complement, and coagulation cascade as CSF signature of cortical lesions in early multiple sclerosis. *Ann Clin Transl Neurol*. 2019;6(11):2150–2163.
- Akassoglou K, Yu W-M, Akpınar P, Strickland S. Fibrin inhibits peripheral nerve regeneration by arresting Schwann cell differentiation. *Neuron*. 2002;33:861–875.
- Pous L, Deshpande SS, Nath S, et al. Fibrinogen induces neural stem cell differentiation into astrocytes in the subventricular zone via BMP signaling. *Nat Commun*. 2020;11(1):630.
- Ryu JK, Petersen MA, Murray SG, et al. Blood coagulation protein fibrinogen promotes autoimmunity and demyelination via chemokine release and antigen presentation. *Nat Commun*. 2015;6:8164.
- Mendiola AS, Ryu JK, Bardehle S, et al. Transcriptional profiling and therapeutic targeting of oxidative stress in neuroinflammation. *Nat Immunol*. 2020;21(5):513–524.
- Back SA, Gan X, Li Y, Rosenberg PA, Volpe JJ. Maturation-dependent vulnerability of oligodendrocytes to oxidative stress-induced death caused by glutathione depletion. *J Neurosci*. 1998;18(16):6241–6253.
- Miron VE, Boyd A, Zhao JW, et al. M2 microglia and macrophages drive oligodendrocyte differentiation during CNS remyelination. *Nat Neurosci*. 2013;16(9):1211–1218.
- Dimou L, Gallo V. NG2-glia and their functions in the central nervous system. *Glia*. 2015;63(8):1429–1451.
- Davalos D, Ryu JK, Merlini M, et al. Fibrinogen-induced perivascular microglial clustering is required for the development of axonal damage in neuroinflammation. *Nat Commun*. 2012;3:1227.
- Adams RA, Bauer J, Flick MJ, et al. The fibrin-derived gamma377–395 peptide inhibits microglia activation and suppresses relapsing paralysis in central nervous system autoimmune disease. *J Exp Med*. 2007;204(3):571–582.
- Ryu JK, Rafalski VA, Meyer-Franke A, et al. Fibrin-targeting immunotherapy protects against neuroinflammation and neurodegeneration. *Nat Immunol*. 2018;19(11):1212–1223.
- Niu J, Tsai HH, Hoi KK, et al. Aberrant oligodendroglial-vascular interactions disrupt the blood-brain barrier, triggering CNS inflammation. *Nat Neurosci*. 2019;22(5):709–718.
- Romanelli E, Sorbara CD, Nikić I, Dagkalis A, Misgeld T, Kerschensteiner M. Cellular, subcellular and functional in vivo labeling of the spinal cord using vital dyes. *Nat Protoc*. 2013;8(3):481–490.
- Falcao AM, van Bruggen D, Marques S, et al. Disease-specific oligodendrocyte lineage cells arise in multiple sclerosis. *Nat Med*. 2018;24(12):1837–1844.
- Kirby L, Jin J, Cardona JG, et al. Oligodendrocyte precursor cells present antigen and are cytotoxic targets in inflammatory demyelination. *Nat Commun*. 2019;10(1):3887.
- Wood JP, Ellery PE, Maroney SA, Mast AE. Biology of tissue factor pathway inhibitor. *Blood*. 2014;123(19):2934–2943.

34. Hackett AR, Yahn SL, Lyapichev K, et al. Injury type-dependent differentiation of NG2 glia into heterogeneous astrocytes. *Exp Neurol*. 2018;308:72–79.
35. Mabie PC, Mehler MF, Marmur R, Papavasiliou A, Song Q, Kessler JA. Bone morphogenetic proteins induce astroglial differentiation of oligodendroglial-astroglial progenitor cells. *J Neurosci*. 1997;17(11):4112–4120.
36. Hao J, Ho JN, Lewis JA, et al. In vivo structure-activity relationship study of dorsomorphin analogues identifies selective VEGF and BMP inhibitors. *ACS Chem Biol*. 2010;5(2):245–253.
37. Green AJ, Gelfand JM, Cree BA, et al. Clemastine fumarate as a remyelinating therapy for multiple sclerosis (ReBUILD): a randomised, controlled, double-blind, crossover trial. *Lancet*. 2017;390(10111):2481–2489.
38. Costa C, Eixarch H, Martinez-Saez E, et al. Expression of bone morphogenetic proteins in multiple sclerosis lesions. *Am J Pathol*. 2019;189(3):665–676.
39. Mohedas AH, Xing X, Armstrong KA, Bullock AN, Cuny GD, Yu PB. Development of an ALK2-biased BMP type I receptor kinase inhibitor. *ACS Chem Biol*. 2013;8(6):1291–1302.
40. Tsai HH, Niu J, Munji R, et al. Oligodendrocyte precursors migrate along vasculature in the developing nervous system. *Science*. 2016;351(6271):379–384.
41. Chavali M, Ulloa-Navas MJ, Perez-Borreda P, et al. Wnt-dependent oligodendroglial-endothelial interactions regulate white matter vascularization and attenuate injury. *Neuron*. 2020;108(6):1130–1145.e5.
42. Ziliotto N, Bernardi F, Jakimovski D, Zivadinov R. Coagulation pathways in neurological diseases: Multiple sclerosis. *Front Neurol*. 2019;10:409.
43. Schachtrup C, Ryu JK, Helmrick MJ, et al. Fibrinogen triggers astrocyte scar formation by promoting the availability of active TGF-beta after vascular damage. *J Neurosci*. 2010;30(17):5843–5854.
44. Pendleton JC, Shambloot MJ, Gary DS, et al. Chondroitin sulfate proteoglycans inhibit oligodendrocyte myelination through PTPsigma. *Exp Neurol*. 2013;247:113–121.
45. Segel M, Neumann B, Hill MFE, et al. Niche stiffness underlies the ageing of central nervous system progenitor cells. *Nature*. 2019;573(7772):130–134.
46. Baror R, Neumann B, Segel M, et al. Transforming growth factor-beta renders ageing microglia inhibitory to oligodendrocyte generation by CNS progenitors. *Glia*. 2019;67(7):1374–1384.
47. Cunniffe N, Coles A. Promoting remyelination in multiple sclerosis. *J Neurol*. 2021;268(1):30–44.
48. Akassoglou K. The immunology of blood: Connecting the dots at the neurovascular interface. *Nat Immunol*. 2020;21(7):710–712.
49. Browning LM, Miller C, Kuczma M, et al. Bone morphogenetic proteins are immunoregulatory cytokines controlling FOXP3(+) Treg cells. *Cell Rep*. 2020;33(1):108219.
50. Yoshioka Y, Ono M, Osaki M, Konishi I, Sakaguchi S. Differential effects of inhibition of bone morphogenetic protein (BMP) signaling on T-cell activation and differentiation. *Eur J Immunol*. 2012;42(3):749–759.
51. Pluchino S, Zanotti L, Brambilla E, et al. Immune regulatory neural stem/precursor cells protect from central nervous system autoimmunity by restraining dendritic cell function. *PLoS One*. 2009;4(6):e5959.
52. Chen W, Ten Dijke P. Immunoregulation by members of the TGFbeta superfamily. *Nat Rev Immunol*. 2016;16(12):723–740.
53. Kan L, Kitterman JA, Procissi D, et al. CNS demyelination in fibrodysplasia ossificans progressiva. *J Neurol*. 2012;259(12):2644–2655.